

Universal prethermal dynamics of Bose gases quenched to unitarity

Christoph Eigen^{1*}, Jake A. P. Glidden¹, Raphael Lopes^{1,5}, Eric A. Cornell^{2,3}, Robert P. Smith^{1,4} & Zoran Hadzibabic^{1*}

Understanding strongly correlated phases of matter, such as the quark–gluon plasma and neutron stars, and in particular the dynamics of such systems, for example, following a Hamiltonian quench (a sudden change in some Hamiltonian parameter, such as the strength of interparticle interactions) is a fundamental challenge in modern physics. Ultracold atomic gases are excellent quantum simulators for these problems, owing to their tunable interparticle interactions and experimentally resolvable intrinsic timescales. In particular, they provide access to the unitary regime, in which the interactions are as strong as allowed by quantum mechanics. This regime has been extensively studied in Fermi gases^{1,2}. The less-explored unitary Bose gases^{3–11} offer possibilities¹² such as universal physics controlled solely by the gas density^{13,14} and new forms of superfluidity^{15–17}. Here, through momentum- and time-resolved studies, we explore degenerate and thermal homogeneous Bose gases quenched to unitarity. In degenerate samples, we observe universal post-quench dynamics in agreement with the emergence of a prethermal state^{18–24} with a universal non-zero condensed fraction^{22,24}. In thermal gases, the dynamic and thermodynamic properties generally depend on the gas density and the temperature, but we find that they can still be expressed in terms of universal dimensionless functions. Surprisingly, we find that the total quench-induced correlation energy is independent of the gas temperature. These measurements provide quantitative benchmarks and challenges for the theory of unitary Bose gases.

In ultracold atomic gases, two-body contact interactions are characterized by the *s*-wave scattering length *a*, and the unitary regime is realized in the limit $a \rightarrow \infty$, with *a* tuned using magnetic Feshbach resonances²⁵. In Bose gases, tuning *a* to infinity also enhances three-body recombination, which leads to particle loss and heating, making unitary Bose gases inherently dynamic, non-equilibrium systems. Experimentally, these systems are studied by rapidly quenching *a* to infinity (Fig. 1a), which initiates the non-equilibrium dynamics. If starting with a Bose–Einstein condensate (BEC) in the $k \approx 0$ momentum state, after the quench the momentum distribution broadens (the kinetic energy increases) owing to lossless correlation dynamics and to recombination heating (Fig. 1b). The interplay between these two processes raises many questions, such as whether the gas attains a strongly correlated quasi-equilibrium steady state before degeneracy is lost.

The timescales of the different processes are set by the natural length scales of the system. Within the universality hypothesis¹⁴, in a homogeneous degenerate unitary gas the only relevant length scale is the interparticle spacing $n^{-1/3}$, where *n* is the particle density, which (in analogy with Fermi gases) sets the Fermi momentum $\hbar k_n = \hbar(6\pi^2 n)^{1/3}$, energy $E_n = \hbar^2 k_n^2 / (2m)$ and time $t_n = \hbar/E_n$, where *m* is the particle mass and \hbar is the reduced Planck constant. Additional, potentially relevant length scales are the sizes of the Efimov trimer states that exist as a result of resonant two-body interactions^{17,26–31}. Three-body correlations⁸ and Efimov trimers⁹ have been observed experimentally, but all

degenerate-gas dynamics have been consistent with t_n being the only characteristic timescale^{6,9,10}. This universality has so far made it impossible to disentangle the lossless from the recombination-induced dynamics. Experimental evidence has suggested that the lossless processes are faster, sufficiently so that the gas attains a degenerate steady state^{6,10}; however, almost nothing could be established about the nature of this state. Here we isolate the effects of the lossless post-quench dynamics through momentum- and time-resolved studies of degenerate and thermal Bose gases.

We prepare a homogeneous ³⁹K Bose gas in an optical-box trap¹⁰ with a volume of around $3 \times 10^4 \mu\text{m}^3$ and use a Feshbach resonance centred at $8\,402.70(3)$ G. Initially, we prepare either a quasi-pure BEC or a thermal gas. In both cases, we start with a weakly interacting system, with $na^3 < 10^{-4}$, then quench the gas to unitarity (within $2 \mu\text{s}$) and let it evolve for a time t_{hold} in our box trap, t_n is a global variable and after the quench all parts of the system evolve in the same way. After the time t_{hold} , we quench the gas back to low *a*, release it from

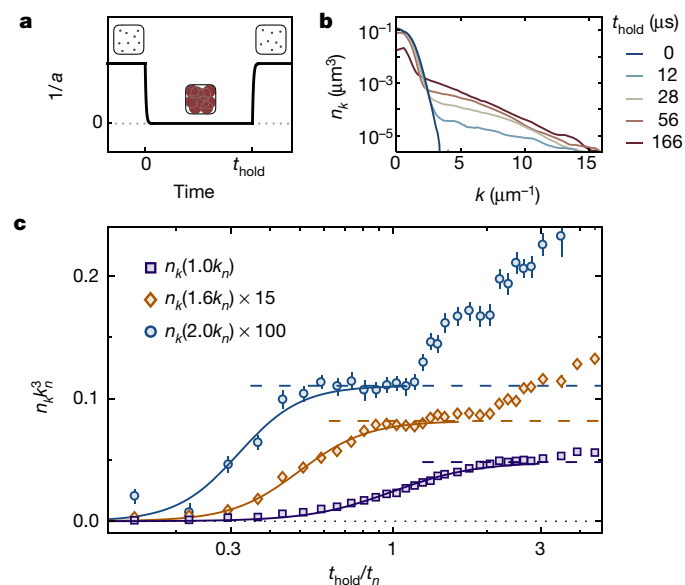


Fig. 1 | Dynamics of a degenerate Bose gas quenched to unitarity. **a**, Quench protocol. The red circles depict atoms, and their sizes the interaction strength, which is limited at unitarity by the interparticle spacing; *a* is the *s*-wave scattering length and t_{hold} is the hold time at unitarity. **b**, Momentum distribution $n_k(k)$ for different t_{hold} values; the initial gas density is $n = 5.1 \mu\text{m}^{-3}$, corresponding to a Fermi momentum of $k_n = 6.7 \mu\text{m}^{-1}$ and a Fermi time of $t_n = 27 \mu\text{s}$. **c**, Populations of individual *k* states show rapid initial growth, saturation at (quasi-)steady-state values of $\bar{n}_k(k)$ (dashed lines) and long-time heating. The error bars reflect 1 s.e.m. (not visible when smaller than the symbol size). The solid lines are sigmoid fits used to extract the initial-growth half-way times $\tau(k)$.

¹Cavendish Laboratory, University of Cambridge, Cambridge, UK. ²JILA, National Institute of Standards and Technology, University of Colorado, Boulder, CO, USA. ³Department of Physics, University of Colorado, Boulder, CO, USA. ⁴Clarendon Laboratory, University of Oxford, Oxford, UK. ⁵Present address: Laboratoire Kastler Brossel, Collège de France, CNRS, ENS-PSL University, UPMC-Sorbonne Université, Paris, France. *e-mail: ce330@cam.ac.uk; zh10001@cam.ac.uk

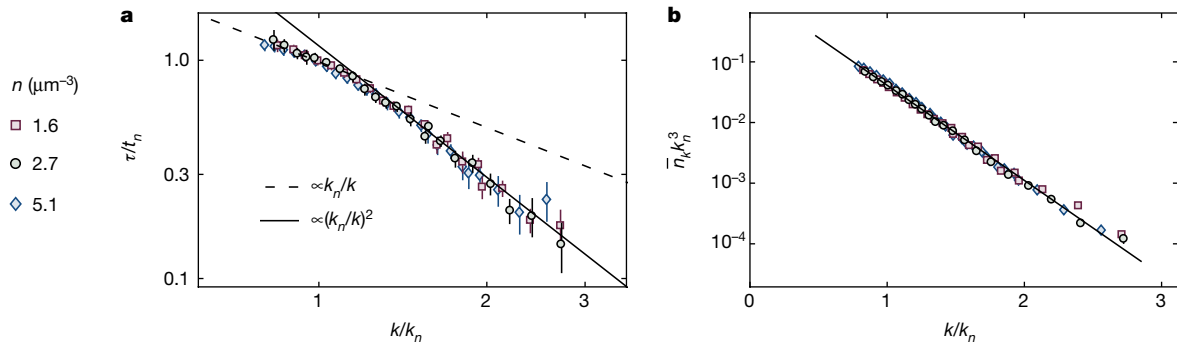


Fig. 2 | Universal post-quench dynamics and the steady-state momentum distribution in the degenerate Bose gas. a, b, The momentum-dependent half-way time $\tau(k)$ for reaching the steady state (a) and the steady-state momentum distribution $\bar{n}_k(k)$ (b), for three different BEC densities n . Expressing all quantities in dimensionless form, using the

trap and measure its momentum distribution $n_k(k)$; we normalize n_k so that

$$\int 4\pi k^2 n_k dk = 1$$

See Methods for further experimental details.

We first present our study of degenerate gases. In Fig. 1b we show $n_k(k)$ for an initial BEC density of $n = 5.1 \mu\text{m}^{-3}$ and various t_{hold} . In Fig. 1c we illustrate our key experimental observation. By looking at n_k values for individual k states, we discern separate stages in the evolution of n_k : after a rapid initial growth, n_k reaches a (quasi-)steady-state plateau, before the long-time heating takes over. All timescales are of order t_n , but distinguishable. We discern such time separation for $k/k_n \gtrsim 0.8$. For each k in this range, we identify the plateau occupation \bar{n}_k (dashed lines in Fig. 1c) and use sigmoid fits (solid lines) to extract the characteristic time $\tau(k)$ for the initial rapid growth of n_k , defined such that $n_k(k, \tau(k)) = \bar{n}_k(k)/2$. We note that t_n and k_n correspond to the initial n ; for our longest τ we observe particle loss of approximately 20%.

In Fig. 1c we also see that the curves for different k values are not aligned in time; $n_k(2k_n)$ shows signs of heating before $n_k(k_n)$ reaches its steady-state value. This finding illustrates why lossless and recombination dynamics could not be separated quantitatively by considering all k at the same evolution time^{6,10}, such as by looking at the kinetic energy per particle $E(t_{\text{hold}})$ ¹⁰. Instead, we separately obtain \bar{n}_k for different k values and piece together the function $\bar{n}_k(k)$. Doing so does not give the momentum distribution at any specific time, but allows us to infer what the steady-state $n_k(k)$ would be if the gas did not suffer from losses and heating. We assume that at early times ($t_{\text{hold}} = \mathcal{O}(t_n)$), all non-zero- k states are primarily fed from the macroscopically occupied BEC (Fig. 1b).

In Fig. 2 we plot the dimensionless τ/t_n and $\bar{n}_k k_n^3$ versus the dimensionless k/k_n , for three BEC densities. By expressing all quantities in dimensionless form, all of our data fall onto universal curves (within experimental errors).

In the experimentally accessible range of momenta, our data are consistent with the scaling $\tau/t_n \propto k_n/k$ at low k and $\tau/t_n \propto (k_n/k)^2$ at high k . These scalings were predicted for the emergence of a prethermal steady state^{20–24}. According to this prediction, at short times after the quench, the excitations are similar to the Bogoliubov modes in a weakly interacting BEC—which are phonons at low k and particles at high k —but with the usual mean-field energy replaced by an energy of order E_n . The speed of sound is then of order $\hbar k_n/m$ and the crossover between the two regimes is at $k = \mathcal{O}(k_n)$. Finally, $\tau(k)$ is set by the dephasing time, which is given approximately by the inverse of the excitation energy.

The form of the universal $\bar{n}_k k_n^3$ curve was not anticipated and poses a new theoretical challenge. Empirically, over three orders of magnitude

Fermi time t_n and momentum k_n as the natural scales, collapses all of our data onto universal curves. The error bars show fitting errors (not visible when smaller than the symbol size). The solid line in b is an exponential fit, $\bar{n}_k k_n^3 = 1.53 \exp(-3.62k/k_n)$.

of $\bar{n}_k k_n^3$, our data are well captured by a simple exponential, $A \exp(-Bk/k_n)$, with $A = 1.53(5)$ and $B = 3.62(2)$ (where the errors are 1σ fitting errors). This function implies a condensed fraction of

$$\eta = 1 - \int 4\pi k^2 \bar{n}_k dk = 19(4)\%$$

Up to $k \approx 3k_n$ we do not observe the asymptotic form $n_k \sim 1/k^4$ that is expected³² at very high k ; however, even if n_k changed to this more slowly decaying form immediately outside of our experimental range, η would change by less than 3%. Previous theoretical work^{22,24} has predicted values of η in the prethermal state that are close to our estimate, but the exponential form of $\bar{n}_k k_n^3$ has not previously been predicted. Explaining this experimental observation may require explicit consideration of the quench back to low a .

We now turn to thermal gases, which reveal some simplifications, but also more surprises. A simplification is that, while in a thermal gas the three-body recombination and the lossless dynamics are both slowed down compared to the degenerate-gas case, the three-body recombination is slowed down more^{4,5,33}. As shown in Fig. 3a, now $E(t_{\text{hold}})$ exhibits two separate stages in the post-quench dynamics: a rapid initial growth (here for $t_{\text{hold}} \lesssim 100 \mu\text{s}$) and long-time heating (for $t_{\text{hold}} \gg 100 \mu\text{s}$). The shape of the curve is similar to those for individual k states in Fig. 1c and the long-time energy growth matches the theory of recombination heating^{4,10}. These results reinforce our interpretation of the two-step dynamics, both for degenerate and for thermal gases. We now focus on the early-time dynamics. As we show in Fig. 3b, $n_k(k)$ is essentially identical at $60 \mu\text{s}$ and $126 \mu\text{s}$, meaning that on this timescale a steady state is established for all k .

In a thermal gas, even before the quench to unitarity, n_k is substantial for all $k \lesssim 1/\lambda$, where $\lambda = h/\sqrt{2\pi m k_B T}$ is the thermal wavelength, T is the initial temperature (before the quench to unitarity), k_B is the Boltzmann constant and $h = 2\pi\hbar$. We therefore look at the redistribution of particles in k space, in particular, the change $\delta n_k(k)$ with respect to $t_{\text{hold}} = 0$ and the corresponding change $\delta \varepsilon$ in the spectral energy density $\varepsilon = \hbar^2/(2m) \times 4\pi k^4 n_k$. An additional challenge in understanding the thermal-gas case is that we have two relevant length scales, $n^{-1/3}$ and λ , and it is not a priori clear whether the dynamic and thermodynamic properties can be expressed in terms of dimensionless universal functions.

In Fig. 3c we show time-resolved population changes in different spherical shells in k space, $4\pi k^2 \delta n_k$. For some special k_0 (dotted line), the population remains essentially constant. In Fig. 3d we show vertical cuts through Fig. 3c for $k < k_0$, $k = k_0$ and $k > k_0$. Away from k_0 , we use sigmoid fits (solid lines) to extract $\tau(k)$, both for diminishing and for growing populations. Near k_0 we see only a small wiggle in δn_k , to which we cannot assign a single timescale.

In Fig. 3e, f we show $\tau(k)$ and the steady state $\overline{\delta \varepsilon}(k)$ for two different combinations of n and T . The $\overline{\delta \varepsilon}(k)$ curve conveys the

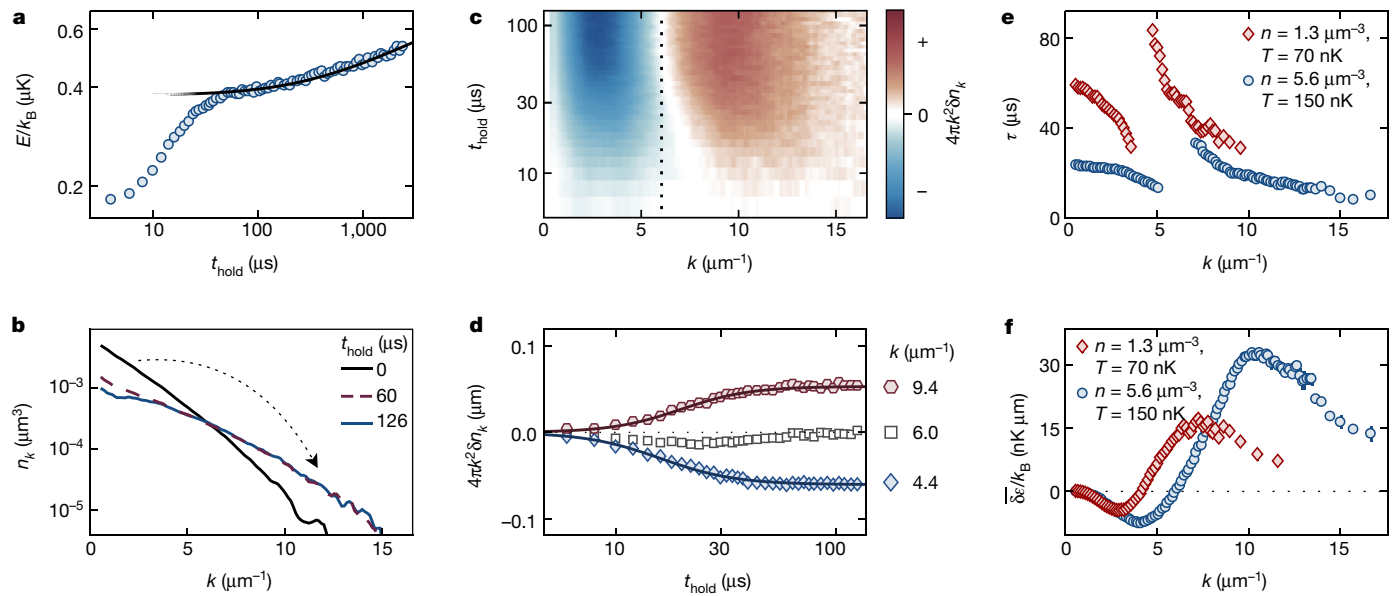


Fig. 3 | Thermal Bose gas quenched to unitarity. **a**, The kinetic energy per particle E shows rapid growth for $t_{\text{hold}} \lesssim 100 \mu\text{s}$ and substantial heating only for $t_{\text{hold}} \gg 100 \mu\text{s}$; the black line is the prediction for recombination heating. Here, and in **b–d**, the initial gas density and temperature are $n = 5.6 \mu\text{m}^{-3}$ and $T = 150 \text{ nK}$, respectively. **b**, Momentum distribution $n_k(k)$ for different hold times at unitarity. The initial redistribution of particles from low k to high k (indicated by the dotted arrow) is essentially complete within $60 \mu\text{s}$, and n_k is almost identical at $126 \mu\text{s}$ and $60 \mu\text{s}$. **c**, Population changes in different k -space shells, $4\pi k^2 \delta n_k(k)$; the

population in $k_0 = 6.0 \mu\text{m}^{-1}$ (dotted line) remains essentially unchanged. **d**, Vertical cuts through the plot in **c**. Solid lines are sigmoid fits used to extract the half-way time $\tau(k)$. **e**, **f**, $\tau(k)$ and the change in the spectral energy density (between the initial, pre-quench state and the post-quench steady state), $\delta \bar{\varepsilon}(k) \propto k^4 \delta n_k(k)$. Here we show data for $n = 5.6 \mu\text{m}^{-3}$ and $T = 150 \text{ nK}$ (blue) and for $n = 1.3 \mu\text{m}^{-3}$ and $T = 70 \text{ nK}$ (red). For the data in **a** and **d**, 1 s.e.m. error bars are smaller than the symbol size. In **e** and **f**, the error bars (in most cases smaller than the symbol size) show fitting errors.

redistribution of particles from $k < k_0$ to $k > k_0$ and the resulting energy growth

$$\overline{\Delta E} = \int \delta \bar{\varepsilon} dk$$

The dispersive shape of $\tau(k)$ was not anticipated and invites further theoretical work. Here, we empirically investigate whether these curves can be scaled into universal dimensionless functions.

For the horizontal scaling we find that the natural scale for k is $1/\lambda$, independent of n . In Fig. 4a we plot $\tau(k)$ versus $k\lambda$, for 15 combinations of n and T (corresponding to phase-space densities $n\lambda^3$ between 0.2 and 2). Similarly, in Fig. 4d we plot $\delta \bar{\varepsilon}(k)/\lambda$ versus $k\lambda$, so that the area under each curve is still $\overline{\Delta E}(n, T)$. In both cases, we see horizontal alignment of all of the curves, with $k_0 = 4.4/\lambda$.

A more challenging question is whether these n - and T -dependent curves may be collapsed vertically, by scaling them by some time

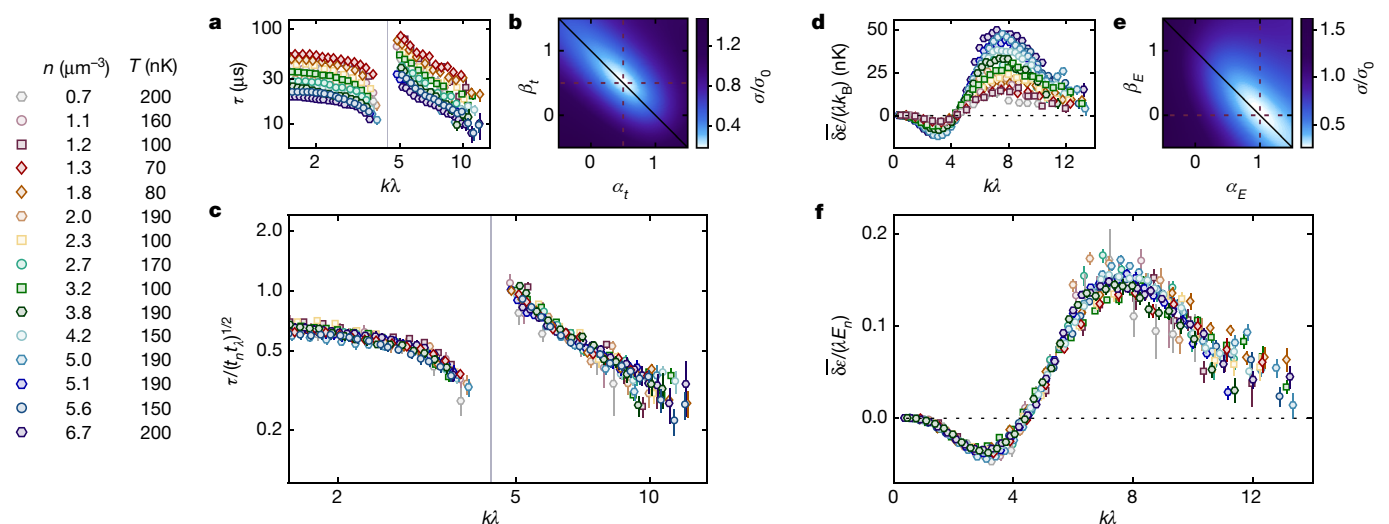


Fig. 4 | Universal dynamic and thermodynamic functions for the thermal Bose gas quenched to unitarity. **a**, **d**, Plotting the half-way time τ for reaching the post-quench steady state (**a**) and the change in the spectral energy density $\delta \bar{\varepsilon}/\lambda$ (where λ is the thermal wavelength; **d**) versus $k\lambda$ horizontally aligns all of our curves for 15 different combinations of the initial gas density n and temperature T (see key). The vertical grey line corresponds to k_0 . **b**, Supposing that the characteristic timescale for the dynamics is $t_s \propto t_n^{\alpha_t} t_\lambda^{\beta_t}$, where $t_\lambda = \hbar/(k_B T)$, we obtain the best data collapse,

corresponding to the minimum of σ/σ_0 (see text for details), for $\alpha_t \approx \beta_t \approx 1/2$ (dashed cross indicates $\alpha_t = \beta_t = 1/2$). This suggests that $t_s \approx \sqrt{t_n t_\lambda}$. **e**, Similarly, for the energy scale $E_s \propto E_n^{\alpha_E} (k_B T)^{\beta_E}$, we find $\alpha_E \approx 1$ and $\beta_E \approx 0$, which suggests that $E_s = E_n$. **c**, **f**, The dimensionless $\tau/\sqrt{t_n t_\lambda}$ (**c**) and $\delta \bar{\varepsilon}/(\lambda E_n)$ (**f**) are, to within experimental errors, universal functions of the dimensionless $k\lambda$. All error bars (not visible when smaller than the symbol size) show fitting errors.

$t_s(n, T)$ and energy $E_s(n, T)$. We conjecture that $t_s \propto t_n^{\alpha_t} t_\lambda^{\beta_t}$, where $t_\lambda = \hbar / (k_B T)$, and similarly $E_s \propto E_n^{\alpha_E} (k_B T)^{\beta_E}$, and determine for which $\alpha_{t,E}$ and $\beta_{t,E}$ we get the best collapse. We treat $\alpha_{t,E}$ and $\beta_{t,E}$ as independent, but physically (if there are no other relevant scales) we expect $\alpha_t + \beta_t = \alpha_E + \beta_E = 1$.

We quantify the degree of the data collapse by a single number σ , which is obtained by calculating the standard deviation of the data for all n and T at a fixed $k\lambda$ and then summing over $k\lambda$. In Fig. 4b, e, we show plots of σ/σ_0 for τ and $\delta\varepsilon/\lambda$; here, σ_0 corresponds to no scaling.

For the temporal scaling, in Fig. 4b we find the lowest σ near $\alpha_t = \beta_t = 1/2$, which suggests that $t_s = \sqrt{t_n t_\lambda}$. In Fig. 4c we plot $\tau/\sqrt{t_n t_\lambda}$ and see that all of our data collapse onto a universal curve (within experimental scatter). For this scaling we have an intuitive interpretation. In a thermal gas, particles do not overlap, so to feel the unitary interactions after the quench they must first meet. The t_s that we find, $\sqrt{t_n t_\lambda} \propto n^{-1/3} \lambda m / \hbar$, matches the expected scaling for the characteristic time until meeting, which is given by the ratio of the interparticle spacing $n^{-1/3}$ and the characteristic thermal velocity $\hbar/(m\lambda)$.

In Fig. 4e we find that the optimal values of α_E and β_E are $\alpha_E \approx 1$ and $\beta_E \approx 0$, suggesting that $E_s = E_n$. This scaling implies that, surprisingly, whereas $\delta\varepsilon(k)$ naturally depends on n and T , its integral ΔE is independent of T ; in Fig. 4f we see that this scaling collapses all of our data onto a universal curve.

This lack of T dependence suggests that $\Delta E/E_n$ in a thermal gas should also be equal to \bar{E}/E_n in a degenerate gas (where $\Delta E = \bar{E}$). Bearing in mind the caveat that we do not observe very high- k tails experimentally, from the data in Fig. 4f we estimate that $\Delta E/E_n = 0.7(1)$ for a thermal gas; from the exponential $\bar{n}_k k_n^3$ in Fig. 2b, we obtain a consistent value of $\bar{E}/E_n = 0.74(4)$ for a degenerate gas.

Our experiments establish a comprehensive view of the prethermal dynamics and thermodynamics of homogeneous Bose gases quenched to unitarity, at low and high temperatures. They provide quantitative benchmarks and new questions for the theory of unitary Bose gases. Open problems include explaining the forms of our experimentally observed universal dynamic and thermodynamic functions, and elucidating the connections between these universal features and previously observed signatures^{8,9} of non-universal Efimov physics. Experimentally, an important future challenge is to probe the coherence and the potential superfluid properties of the prethermal state of a degenerate unitary Bose gas.

While this paper was under review, we learned of two other experiments that observe universality in the many-body dynamics of out-of-equilibrium quantum systems^{34,35}.

Online content

Any methods, additional references, Nature Research reporting summaries, source data, statements of data availability and associated accession codes are available at <https://doi.org/10.1038/s41586-018-0674-1>.

Received: 18 May; Accepted: 28 September 2018;

Published online 7 November 2018.

- Zwinger, W. (ed.) *The BCS-BEC Crossover and the Unitary Fermi Gas* (Springer, Berlin, 2011).
- Zwierlein, M. W. in *Novel Superfluids* Vol. 2 (eds Bennemann, K.-H. & Ketterson, J. B.) Ch. 18 (Oxford Univ. Press, Oxford, 2014).
- Navon, N. et al. Dynamics and thermodynamics of the low-temperature strongly interacting Bose gas. *Phys. Rev. Lett.* **107**, 135301 (2011).
- Rem, B. S. et al. Lifetime of the Bose gas with resonant interactions. *Phys. Rev. Lett.* **110**, 163202 (2013).
- Fletcher, R. J., Gaunt, A. L., Navon, N., Smith, R. P. & Hadzibabic, Z. Stability of a Unitary Bose Gas. *Phys. Rev. Lett.* **111**, 125303 (2013).
- Makotyn, P., Klauss, C. E., Goldberger, D. L., Cornell, E. A. & Jin, D. S. Universal dynamics of a degenerate unitary Bose gas. *Nat. Phys.* **10**, 116–119 (2014).
- Eismann, U. et al. Universal loss dynamics in a unitary Bose gas. *Phys. Rev. X* **6**, 021025 (2016).
- Fletcher, R. J. et al. Two- and three-body contacts in the unitary Bose gas. *Science* **355**, 377–380 (2017).

- Klauss, C. E. et al. Observation of Efimov molecules created from a resonantly interacting Bose gas. *Phys. Rev. Lett.* **119**, 143401 (2017).
- Eigen, C. et al. Universal scaling laws in the dynamics of a homogeneous unitary Bose gas. *Phys. Rev. Lett.* **119**, 250404 (2017).
- Fletcher, R. J. et al. Elliptic flow in a strongly interacting normal Bose gas. *Phys. Rev. A* **98**, 011601 (2018).
- Chevy, F. & Salomon, C. Strongly correlated Bose gases. *J. Phys. B* **49**, 192001 (2016).
- Cowell, S. et al. Cold Bose gases with large scattering lengths. *Phys. Rev. Lett.* **88**, 210403 (2002).
- Ho, T.-L. Universal thermodynamics of degenerate quantum gases in the unitarity limit. *Phys. Rev. Lett.* **92**, 090402 (2004).
- Radzihovsky, L., Park, J. & Weichman, P. B. Superfluid transitions in bosonic atom-molecule mixtures near a Feshbach resonance. *Phys. Rev. Lett.* **92**, 160402 (2004).
- Romans, M. W. J., Duine, R. A., Sachdev, S. & Stoof, H. T. C. Quantum phase transition in an atomic Bose gas with a Feshbach resonance. *Phys. Rev. Lett.* **93**, 020405 (2004).
- Piatecki, S. & Krauth, W. Efimov-driven phase transitions of the unitary Bose gas. *Nat. Commun.* **5**, 3503 (2014).
- Berges, J., Borsányi, Sz. & Wetterich, C. Prethermalization. *Phys. Rev. Lett.* **93**, 142002 (2004).
- Gring, M. et al. Relaxation and prethermalization in an isolated quantum system. *Science* **337**, 1318–1322 (2012).
- Yin, X. & Radzihovsky, L. Quench dynamics of a strongly interacting resonant Bose gas. *Phys. Rev. A* **88**, 063611 (2013).
- Sykes, A. G. et al. Quenching to unitarity: quantum dynamics in a three-dimensional Bose gas. *Phys. Rev. A* **89**, 021601 (2014).
- Kain, B. & Ling, H. Y. Nonequilibrium states of a quenched Bose gas. *Phys. Rev. A* **90**, 063626 (2014).
- Rançon, A. & Levin, K. Equilibrating dynamics in quenched Bose gases: characterizing multiple time regimes. *Phys. Rev. A* **90**, 021602 (2014).
- Yin, X. & Radzihovsky, L. Postquench dynamics and prethermalization in a resonant Bose gas. *Phys. Rev. A* **93**, 033653 (2016).
- Chin, C., Grimm, R., Julienne, P. & Tiesinga, E. Feshbach resonances in ultracold gases. *Rev. Mod. Phys.* **82**, 1225–1286 (2010).
- Efimov, V. Energy levels arising from resonant two-body forces in a three-body system. *Phys. Lett. B* **33**, 563–564 (1970).
- Kraemer, T. et al. Evidence for Efimov quantum states in an ultracold gas of caesium atoms. *Nature* **440**, 315–318 (2006).
- Smith, D. H., Braaten, E., Kang, D. & Platter, L. Two-body and three-body contacts for identical bosons near unitarity. *Phys. Rev. Lett.* **112**, 110402 (2014).
- Comparin, T. & Krauth, W. Momentum distribution in the unitary Bose gas from first principles. *Phys. Rev. Lett.* **117**, 225301 (2016).
- Colussi, V. E., Corson, J. P. & D'Incao, J. P. Dynamics of three-body correlations in quenched unitary Bose gases. *Phys. Rev. Lett.* **120**, 100401 (2018).
- D'Incao, J. P., Wang, J. & Colussi, V. E. Efimov physics in quenched unitary Bose gases. *Phys. Rev. Lett.* **121**, 023401 (2018).
- Tan, S. Energetics of a strongly correlated Fermi gas. *Ann. Phys.* **323**, 2952–2970 (2008).
- Li, W. & Ho, T.-L. Bose gases near unitarity. *Phys. Rev. Lett.* **108**, 195301 (2012).
- Prüfer, M. et al. Observation of universal dynamics in a spinor Bose gas far from equilibrium. *Nature* <https://doi.org/10.1038/s41586-018-0659-0> (2018).
- Erne, S., Bucker, R., Gasenzer, T., Berges, J. & Schmiedmayer, J. Universal dynamics in an isolated one-dimensional Bose gas far from equilibrium. *Nature* <https://doi.org/10.1038/s41586-018-0667-0> (2018).

Acknowledgements We thank R. Fletcher, N. Navon and T. Hilker for discussions and comments on the manuscript. This work was supported by the Royal Society, EPSRC (grant numbers EP/N011759/1 and EP/P009565/1), ERC (QBox), AFOSR and ARO. R.L. acknowledges support from the EU Marie Curie programme (grant number MSCA-IF-2015 704832) and Churchill College, Cambridge. E.A.C. acknowledges hospitality and support from Trinity College, Cambridge.

Reviewer information Nature thanks M. Kolodrubetz and the other anonymous reviewer(s) for their contribution to the peer review of this work.

Author contributions C.E., J.A.P.G. and R.L. collected the data. C.E. analysed the data and produced the figures. C.E., E.A.C., R.P.S. and Z.H. interpreted the data and wrote the manuscript.

Competing interests The authors declare no competing interests.

Additional information

Extended data is available for this paper at <https://doi.org/10.1038/s41586-018-0674-1>.

Reprints and permissions information is available at <http://www.nature.com/reprints>.

Correspondence and requests for materials should be addressed to C.E. or Z.H. **Publisher's note:** Springer Nature remains neutral with regard to jurisdictional claims in published maps and institutional affiliations.

METHODS

Optical-box trap and sample preparation. As described previously^{36,37}, our box trap is formed by blue-detuned, 532-nm laser beams. It is cylindrical in shape, with a diameter of about 30 μm and a length of about 45 μm . We deduce n from the measured atom number, and take into account the fact that the trap walls are not infinitely steep³⁶, owing to the diffraction limit on the sharpness of the laser beams, so the effective trap volume depends slightly on the energy per particle in the initially prepared sample.

Our clouds are in the lowest hyperfine ground state and we initially prepare them at a field of approximately 399.1 G. At this field, the scattering length is $a_i \approx 400a_0$, where a_0 is the Bohr radius.

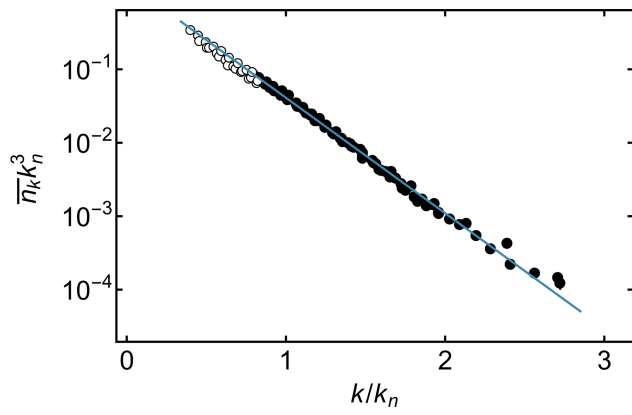
Quench protocol and measurement details. At the end of t_{hold} we quench a back to a_i using an exponential field ramp with a time constant of 1 μs . We use the fastest ramp that is technically possible to minimize the conversion of atoms into molecules^{9,10}. We then release the gas from the trap and simultaneously (within about 3 ms) completely turn off interactions ($a \rightarrow 0$). After letting the cloud expand for 6–12 ms of time of flight, we take an absorption image of it. We typically repeat each measurement about 20 times. To reconstruct $n_k(k)$ from the two-dimensional absorption images, which give the momentum distribution integrated along the line of sight, we average each image azimuthally, then average over the experimental repetitions, and finally perform the inverse Abel transform. Owing to the initial cloud size and non-infinite time of flight, our measurements of $n_k(k)$ are not quantitatively reliable for $k < 2 \mu\text{m}^{-1}$.

Extrapolation of $\bar{n}_k k_n^3$ in a degenerate gas. We also use our experimental data to estimate how the function $\bar{n}_k k_n^3$ extrapolates to lower k/k_n , without presuming its functional form. For $k/k_n < 0.8$, we do not see clear steady-state plateaux in $n_k(t_{\text{hold}})$, such as indicated by the dashed lines in Fig. 1c. However, we can extrapolate $\tau \propto t_n k_n/k$ according to the dashed line in Fig. 2a; then, assuming that heating effects are not yet substantial at $t_{\text{hold}} = \tau(k)$ and following our definition of τ , we estimate $\bar{n}_k = 2n_k(\tau)$, where $n_k(\tau)$ is the n_k measured at the extrapolated τ . These extrapolated values of $\bar{n}_k k_n^3$ are shown by open symbols in Extended Data Fig. 1. They fall on the same exponential curve that fits our directly measured values of $\bar{n}_k k_n^3$ (solid symbols), lending further support for this unexpected functional form.

Data availability

The data that support the findings of this study are available in the Apollo repository (<https://doi.org/10.17863/CAM.30242>). Any additional information is available from the corresponding authors on reasonable request.

36. Gaunt, A. L., Schmidutz, T. F., Gotlibovych, I., Smith, R. P. & Hadzibabic, Z. Bose–Einstein condensation of atoms in a uniform potential. *Phys. Rev. Lett.* **110**, 200406 (2013).
37. Eigen, C. et al. Observation of weak collapse in a Bose–Einstein condensate. *Phys. Rev. X* **6**, 041058 (2016).



Extended Data Fig. 1 | Extrapolation of $\bar{n}_k k_n^3$ in a degenerate gas to lower k/k_n . Solid symbols show directly measured values (also shown in Fig. 2b), here combining the data for all three BEC densities. Open symbols show experimentally extrapolated values, for all three densities, as described in Methods. The solid line is the same as in Fig. 2b.